CALIOP Algorithm Theoretical Basis Document

Part 1 : CALIOP Instrument, and Algorithms Overview

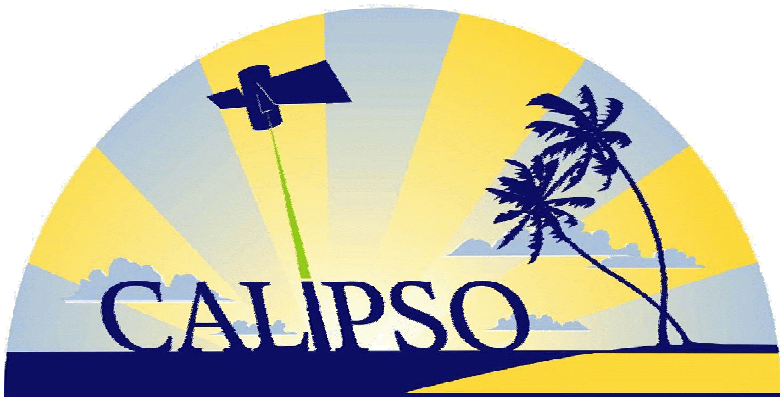

Primary Authors:

David M. Winker, NASA Langley Research Center
Chris A. Hostetler, NASA Langley Research Center
Mark A. Vaughan, Science Applications International Corp. (SAIC)
Ali H. Omar, NASA Langley Research Center

PC-SCI-202 Part 1

Release 2.0

September 9, 2006

CALIOP Algorithm Theoretical Basis Document

Part 1 : CALIOP Instrument, and Algorithms Overview

Prepared by

Ali H. Omar 09/08/2006

Approved by

David M. Winker 10/03/2006
CALIPSO Principal Investigator

Table of Contents

1. Introduction

CALIPSO (Cloud-Aerosol Lidar and Infrared Pathfinder Satellite Observations) is a joint NASA-CNES satellite mission designed to provide measurements aimed at improving our understanding of the role of aerosols and clouds in the climate system. The Cloud-Aerosol LIdar with Orthogonal Polarization (CALIOP, pronounced the same as "calliope") is the primary instrument on the CALIPSO satellite. CALIOP, built by Ball Aerospace and Technologies Corporation, Fibertek, and NASA's Langley Research Center (LaRC), is designed to acquire vertical profiles of elastic backscatter at two wavelengths (1064 nm and 532 nm) from a near nadir-viewing geometry during both day and night phases of the orbit. In addition to the total backscatter at the two wavelengths, CALIOP also provides profiles of linear depolarization at 532 nm. Accurate aerosol and cloud heights and the retrieval of extinction coefficient profiles are be derived from the total backscatter measurements. The depolarization measurements enable the discrimination between ice clouds and water clouds and the identification of non-spherical aerosol particles. Additional information, such as estimates of aerosol particle size, are obtained from the ratios of the signals obtained at the two wavelengths. In addition to CALIOP, the CALIPSO satellite payload includes an Imaging Infrared Radiometer (IIR), provided by CNES, with three channels in the infrared region optimized for retrievals of cirrus particle size, and a single channel Wide Field Camera (WFC). The WFC is a moderate spatial resolution camera operating in the visible regime to provide meteorological context for CALIOP and IIR measurements, and as a means of accurately co-registering CALIPSO observations to those from other instruments in the A-Train such as MODIS (MODerate Resolution Imaging Spectroradiometer). WFC data is also combined with data from the IIR and CALIOP to retrieve cloud properties. The A-Train is a constellation of United States and international Earth science satellites that fly together with EOS Aqua to enable coordinated science observations. These satellites have an afternoon crossing time close to the mean local time of the 'lead' satellite, Aqua (1:30 p.m.); thus, the name, 'A (short for afternoon) Train'. On April 28, 2006, the CALIPSO satellite was launched to a low earth sun-synchronous orbit at a 705-km altitude, and an inclination of 98.2 degrees.

In section 2 of this document, we present an overview of the CALIPSO mission including the scientific objectives and motivation. An overview of the instrument and data acquisition system is presented in section 3. Section 4 deals with the algorithm heritage, and section 5 provides an overview of the CALIOP automated data analysis system. Calibration processing, discussed in section 6, is designed to accomplish two major goals: (1) the determination of calibration constants for the three lidar channels, and (2) the application of those calibration constants to produce the profiles of attenuated backscatter coefficients that are used in Level 2 processing.

Section 7 presents a brief summary of the design of the lidar Level 2 algorithms. The primary data parameters produced by the Level 2 subsystem are: profiles of cloud and aerosol backscatter and extinction coefficients; cloud and aerosol layer heights; and cloud ice/water phase. An exhaustive list of products can be found in the CALIPSO Data Products Catalogue (PC-SCI-503).

1.1. Purpose and Scope

The purpose of this document is to provide a brief description of the CALIOP instrument and an overview of the algorithms used to produce the Level 1 and Level 2 CALIOP data products.

This volume presents the overall architecture of the algorithm design. Details of the calibration algorithms and the algorithms for layer detection, layer identification, and retrieval of profiles are described in other ATBD volumes. Appendix A of these ATBDs (see PC-SCI-202.05) specifies the content and the native output format of the CALIPSO production data processing system. The cloud and aerosol data products distributed to end-users of the CALIPSO data are harvested from the data and file structures described in this appendix.

The Level 1 algorithms section of this document explains how the instrument calibration constants are determined, and attenuated backscatter coefficients at 532 and 1064 nm produced. The Level 2 algorithms section illustrates the generation of geophysical data products using Level 1 lidar data and various meteorological and ancillary data products. Some of the cloud parameters produced are subsequently used by the IIR Level 2 subsystem to produce cloud emissivity and cloud particle size.

The documents referenced in Section 1.2 can be consulted for additional detail on CALIOP algorithms, data products, and plans for validation.

1.2. Related Documents

PC-SCI-201:	CALIOP Algorithm Theoretical Basis Document: Calibration and Level 1 Data Products
PC-SCI-202 Part 1:	CALIOP Algorithm Theoretical Basis Document: CALIOP Instrument, and Algorithms Overview (this document)
PC-SCI-202 Part 2:	CALIOP Algorithm Theoretical Basis Document: Feature detection and layer properties algorithms
PC-SCI-202 Part 3:	CALIOP Algorithm Theoretical Basis Document: Scene classification algorithms
PC-SCI-202 Part 4:	CALIOP Algorithm Theoretical Basis Document: Extinction retrieval and particle property algorithms
PC-SCI-202 Part 5:	CALIOP Algorithm Theoretical Basis Document: Appendices
PC-SCI-501:	CALIPSO Science Validation Plan
PC-SCI-503:	CALIPSO Data Products Catalog
PC-SCI-504:	Quid Pro Quo Validation Plan

1.3. Revision History

The algorithms are described in this document as they have been implemented in the launch build of the CALIPSO production data processing system. Changes will be documented in Table 1.3.

Table 1.3. Revision history of the CALIOP algorithms

Version	Release Date	Comments
0.01	14 July 2006	Initial version

2. Mission Overview

Current uncertainties in the roles played by clouds and aerosols in the Earth radiation budget limit our understanding of the climate system and the potential for global climate change [*IPCC*, 2001]. Aerosols can significantly impact the Earth's radiation budget through scattering and absorption of incoming sunlight. Aerosols can also impact cloud formation and radiative properties, as well as altering precipitation. In heavily polluted regions, aerosols can have deleterious health effects. Unlike greenhouse gases, tropospheric aerosols are highly variable in space and time, and satellite observations are required to understand the distribution and impact of aerosols on regional and global scales.

On the other hand, the response of Earth's climate to the radiative forcing from greenhouse gases and aerosols is largely controlled by the interactions between clouds and radiation [*Cess et al.*, 1995; *Fouquart et al.*, 1990; *Slingo*, 1990; *Twomey*, 1977; *Wielicki et al.*, 1995]. Advances in modeling capabilities to predict climate change require improved representations of cloud processes in models, and decreased uncertainties in cloud-radiation interactions. The largest source of uncertainty in estimating longwave radiative fluxes at the Earth's surface and within the atmosphere arises from current difficulties in determining the vertical distribution and overlap of multi-layer clouds.

The CALIPSO mission builds on the experience of LITE, which flew a three-wavelength lidar on the space shuttle in 1994 [*Winker et al.*, 1996]. CALIPSO enhances our current measurement capabilities with a payload consisting of a two-wavelength polarization-sensitive lidar, and two passive imagers operating in the visible and infrared spectral regions. Data from these instruments are used to measure the vertical distributions of aerosols and clouds in the atmosphere, as well as optical and physical properties of aerosols and clouds which influence the Earth's radiation budget. The CALIPSO mission provides data to address several objectives:

- to improve observationally-based estimates of direct and indirect aerosol radiative forcing,
- to improve characterization of surface longwave radiative fluxes and atmospheric heating rates, and
- to improve model parameterizations of cloud-climate feedbacks.

The overall objective is to improve the representation of aerosols and clouds in models, including climate models, weather forecast models, and air quality models.

The CALIPSO lidar, CALIOP, provides global, vertically-resolved measurements of aerosol distribution and aerosol extinction coefficients, with an ability to perform height-resolved discrimination of aerosol into several types. Unlike the current generation of space-based remote sensing instruments, CALIOP can observe aerosol over bright surfaces and beneath thin clouds as well as in clear sky conditions. Cloud data from CALIOP are incorporated into the IIR retrieval algorithm to reduce uncertainties in the retrieval of cloud emissivity and particle size.

3. Instrument and Data Acquisition Overview

This section provides a summary of the CALIOP instrument and the data acquisition process. Further details can be found in [*Winker et al.*, 2004]. CALIOP consists of a laser transmitter subsystem and a receiver subsystem. Figure 3.1 shows an exploded view of the "lidar core" contained inside the payload housing. The instrument is built around a T-shaped optical bench which assures stability of the transmitter-to-receiver alignment. The lidar receiver telescope is attached to one side of the bench with the receiver optics and detector assemblies on the other side. The laser transmitter assembly is attached to the top of the "T" by a precision linear drive mechanism and gimbal assembly, allowing precise and accurate alignment of the transmitter and receiver.

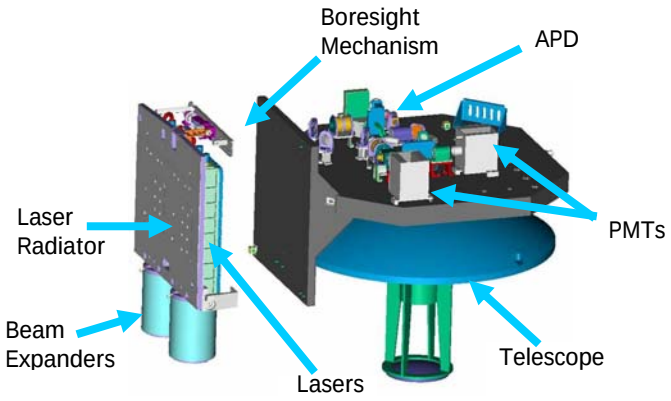

Figure 3.1. CALIOP transmitter and receiver subsystems.

3.1. Transmitter Subsystem

The laser transmitter subsystem includes two identical laser transmitters, each with a beam expander, and a beam steering system that ensures alignment between the transmitter and receiver. The Nd:YAG lasers produce simultaneous pulses at 1064 nm and 532 nm at a pulse repetition rate of 20.16 Hz. The lasers are Q-switched to provide a pulse length of about 20 nsec. Each laser generates 220 mJ of energy at 1064 nm, which is frequency-doubled to produce 110 mJ of energy at each of the two wavelengths. Polarization out-coupling provides a highly polarized output beam. Each laser is housed in its own sealed canister filled with dry air at slightly more than standard atmospheric pressure. The output pulse energy at each wavelength is measured using energy monitors located within each canister. Beam expanders reduce the angular divergence of the transmitted laser beam to produce a beam diameter of 70 meters at the Earth's surface. Transmitter specifications are summarized in Table 3.1.

The lasers were built by Fibertek, Inc. of Herndon, VA, in collaboration with members of the CALIPSO engineering teams at Ball Aerospace and LaRC.

Table 3.1. CALIOP laser specifications

Laser	Diode-pumped Nd:YAG
Pulse Energy	110 mJ @ 532 nm 110 mJ @ 1064 nm
Rep Rate	20.16 Hz
Pulse Length	20 nsec
Linewidth	30 pm
Polarization Purity	> 1000:1 (532 nm)
Beam Divergence	100 μrad (after beam expander)
Boresight Range	±1 degree, 1.6 μrad steps
Laser Environment	18 psia, dry air

3.2. Receiver Subsystem

Shown schematically in Figure 3.2, the receiver sub-system consists of the 1-meter telescope, relay optics, detectors, preamps, and line drivers, all mounted on a stable optical bench. The completed payload is shown in Figure 3.3. Signal processing and control electronics are contained in boxes mounted on the payload housing. The receiver telescope is an all-beryllium 1-meter diameter design similar to the telescope built for the GLAS instrument on the ICESat satellite [*Zwally et al.*, 2002]. The telescope primary mirror, secondary mirror, metering structure, and inner baffle are all made of beryllium, for lightness and to minimize the effect of thermal gradients. A light shade prevents direct solar illumination of the mirrors. The telescope is thermally isolated from the optical bench. A field stop at the focus of the telescope defines the receiver field of view of 130 μrad (full angle) and also rejects stray light. A movable shutter placed downstream from the focus blocks light to allow measurements of detector dark current. The shutter mechanism also allows a pseudo-depolarizer [*McGuire and Chapman*, 1990] to be moved into the 532 nm beam for depolarization calibration. A polarization beamsplitter is used to separate the 532 nm parallel and perpendicular returns. A narrowband etalon is used in combination with a dielectric interference filter in the 532-nm channel to reduce the solar background illumination, while an interference filter alone provides sufficient solar rejection for the 1064 nm channel. Photomultiplier tubes (PMTs) are used for the 532 nm detectors as they provide large linear dynamic range, very low dark noise, and reasonable quantum efficiency. An avalanche photodiode (APD) is used at 1064 nm as PMT detectors have poor quantum efficiency at that wavelength. The APD has good dynamic range and quantum efficiency but the dark noise is much larger than for the PMTs. Thus the 532 nm channels are more sensitive.

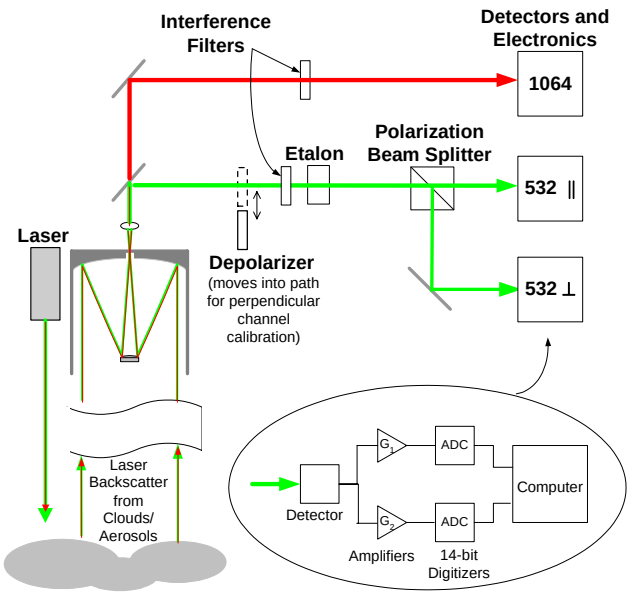

Figure 3.2. Functional block diagram of CALIOP

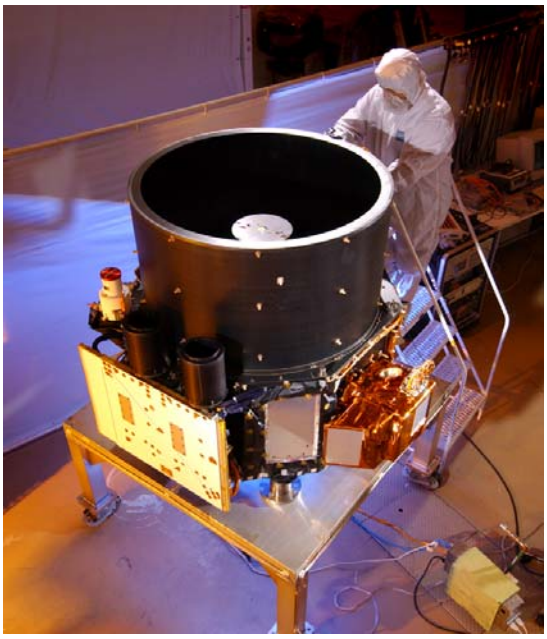

Figure 3.3. Completed CALIOP payload under test in BATC facilities.

CALIOP is required to accurately measure signal returns from the aerosol-free region between 30 km and 35 km as well as the strongest cloud returns. For this reason, all detectors are used in analog mode, although the electronic gains of the 532 nm channels are large enough to allow detection of single photoelectron events. The signal processing electronics have been designed so the linear dynamic range encompasses the full range of molecular, aerosol, and cloud backscattering encountered in the atmosphere, which spans about six orders of magnitude. Dual 14-bit digitizers on each channel provide the effective 22-bit dynamic range which is required. Table 3.2 lists specifications of the receiver subsystem.

Table 3.2 CALIOP receiver parameters

Telescope diameter	1 meter
Field of View	130 μrad
Digitization Rate	10 MHz
Linear Dynamic Range	4 E+6 : 1
532 nm Channel: Detector Etalon Passband Etalon Peak Transmission Blocking Filter	 PMT 37 pm 85% 770 pm
1064 nm Channel: Detector Optical Passband Peak Transmission	 APD 450 pm 84%

3.3. Data Acquisition and Signal Processing

A number of functions are performed by the instrument to convert the analog detector signals into the data which are downlinked. These include range determination, background subtraction, digitization, merging, and averaging. There are two opposing drivers on data processing: to maximize spatial resolution and dynamic range of the signal while minimizing the telemetry data volume. Several features were implemented to reduce the required telemetry bandwidth by more than an order of magnitude relative to the raw data, with minimum impact on the information content of the data.

Due to the oblateness of the Earth, the range from the circular orbit of the CALIPSO satellite to mean sea level (MSL, defined by the height of the geoid) varies by about 21 km through the orbit. The rate of change of the range to MSL is as much as 22 meters/sec. To allow on-orbit averaging of profile data while maintaining the vertical resolution of 30 meters, the data acquisition timing is adjusted to account for the changing range to the Earth's surface. The Payload Controller makes a real-time determination of the range to MSL for each laser shot using an on-board geoid model and an orbit propagator, which is updated using data from the spacecraft GPS. The data acquisition timing is then adjusted so that each profile has the same altitude registration with respect to the geoid.

Data acquisition timing is illustrated in Figure 3.4 in terms of height above MSL. A timer is started when the laser fires. When the laser pulse reaches an altitude of 115 km above MSL, the PMT detectors are gated on and the profile signals from all three channels are acquired (the APD detector has no gate and is always on). The analog profiles are sampled at 10 MHz (corresponding to a 15 m range interval) until the elapsed time corresponds to a range of 18.5 km below sea level, at which point the PMTs are gated off and the digitizers stop sampling. The samples acquired between 40 km (30 km for the 1064 nm channel) and –2 km are used to create the profile data which is downlinked. The portions of the profile above 60 km and below –11 km are used to measure DC signal levels.

During daylight measurements, the solar background signal can be as large as the clear-sky atmospheric signal. The instrument measures the DC background of each profile from the signal acquired between 112 km and 97 km, where the laser backscatter signals are negligible. This DC signal is electronically subtracted from the analog profile before digitization to allow the dynamic range of the digitizer to be used most effectively. This subtraction will result in negative-going noise excursions if the laser backscatter signal is small and these negative spikes will be clipped by the digitizers, biasing the mean signal. To avoid this, a fixed electrical offset is added, prior to digitization, to the portion of the profile below 97 km. The magnitude of this offset is accurately measured using the 1000 samples acquired between 75.3 km and 60.3 km, which are averaged and downlinked as a single value. This average of the upper background region is numerically subtracted from the profile during later processing. The 500 samples between –11 km and –18.5 km are also averaged and downlinked, providing another measure of the offset.

Two 10 MHz 14-bit analog-to-digital converters (ADCs), set for different gains, are used in each channel to provide the required 22-bit effective dynamic range. The high gain ADC is used to measure weak signals, while the low gain ADC is used to acquire those signals which saturate the high gain digitizer. A composite backscatter profile is then generated by using all samples

from the high-gain ADC that remain onscale. In those instances when a sample is saturated on the high-gain ADC, the corresponding sample from the low-gain ADC is used.

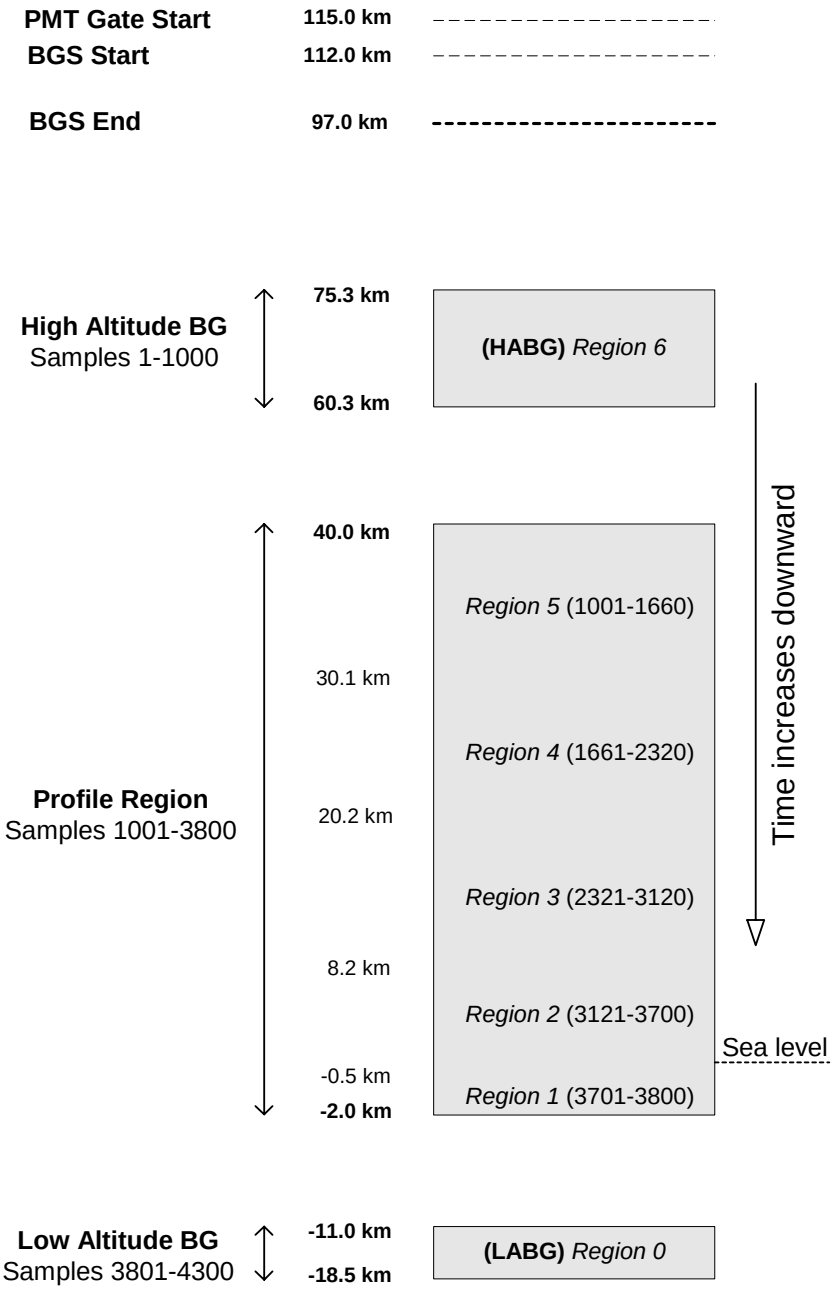

Figure 3.4

Figure 3.4 CALIPSO on-orbit data acquisition timing. Sample numbers refer to the number of 15-meter range bins

The outputs of each pair of digitizers are re-scaled and merged into a single profile before being downlinked. The fundamental sampling resolution of the lidar is 30 meters vertical and 333

meters horizontal, determined by the receiver electrical bandwidth and the laser pulse repetition rate. Therefore, each pair of adjacent 15-meter samples is averaged to produce a profile of 1400 30-meter samples extending from 40 km to -2 km. 1064 nm profiles extend only from 30 km to -2 km, as 1064 nm returns from the purely molecular atmosphere above 30 km are negligibly small.

Table 3.3 Spatial resolutions for the CALIPSO on-board averaging scheme

Altitude Region		Vertical Resolution	Horizontal Resolution	Profiles per 5-km	Samples per Profile
Base (km)	Top (km)				
40.0	30.1	300 meters	5000 meters	1	33
20.2	30.1	180 meters	1667 meters	3	55
8.2	20.2	60 meters	1000 meters	5	200
-0.5	8.2	30 meters	333 meters	15	290
-2.0	-0.5	300 meters	333 meters	15	5

The atmosphere becomes more spatially uniform with increasing altitude. Further, signals from higher in the atmosphere tend to be weaker and require more averaging. Therefore, an altitude-dependent on-board averaging scheme was developed which provides full resolution in the lower troposphere – where the spatial variability of cloud and aerosol is greatest – and lower resolution higher in the atmosphere. The degree of averaging varies with altitude, as detailed in Table 3.3 (altitudes are with respect to mean sea level).

4. Algorithm Heritage

There are number of effective methods for deriving particulate extinction and backscatter coefficients from the calibrated, range-corrected lidar signal. Among these, the most widely used are the Klett method [*Klett*, 1985] the Fernald method [*Fernald*, 1984] and the so-called linear iterative method first introduced in the late 1960s [*Elterman*, 1966] and subsequently used extensively by Platt [*Platt*, 1973; *Platt et al.*, 1998]. Klett and Fernald offer closed form, analytic solutions, while the linear iterative technique is a simple numerical solution. The Klett and Fernald algorithms were both originally developed in the context of single scattering. In later years, both algorithms were adapted for use in multiple scattering analyses using a correction factor to the range-resolved extinction coefficients (e.g., as in [*Young*, 1995]). The CALIPSO algorithms account for multiple scattering by applying a correction factor, derived from the phase functions of the CALIPSO aerosol models [*Omar et al.*, 2004; *Omar et al.*, 2005], to the integrated optical depth.

The majority of the CALIOP Level 2 algorithms are based on experience acquired from the Lidar In-space Technology Experiment (LITE) mission [*Winker et al.*, 1996], albeit with several significant enhancements. The CALIPSO feature-finding algorithm is driven by a profile-scanning engine originally developed for application to ground-based observations [*Winker and Vaughan*, 1994] and later adapted for space-based analyses using LITE data [*Platt et al.*, 1999]. The CALIOP instrument has several significant design differences from LITE, which resulted in modifications of some of the methods used in the LITE algorithms and also provided new

opportunities. The LITE laser operated at three wavelengths (355 nm, 532 nm, and 1064 nm) whereas CALIOP operates only at 532 nm and 1064 nm. The CALIOP receiver is polarization-sensitive at 532 nm, however. The additional information from the CALIOP depolarization channel enables identification of non-spherical aerosol particles and cloud ice/water phase. The LITE receiver had limited dynamic range and was typically operated either in low-gain mode, where sensitivity to aerosol was limited, or in high-gain mode where many cloud returns were saturated. All three CALIOP receiver channels have wide dynamic range, allowing both aerosol and cloud to be measured using a single receiver configuration. For additional information on the LITE instrument and scientific investigations, see *Winker et al.* [1996]. LITE flew on the Space Shuttle and acquired data over a period of 11 days whereas CALIPSO is intended to acquire data over a three-year mission. The requirement to process large volumes of data mandated a degree of automation in the data processing system that was not necessary with LITE. The CALIOP retrieval algorithms also had to be adapted to data with a spatial resolution which varies with altitude (as described in Section 3.3).

5. CALIOP Algorithm Overview

The Level 1 algorithms perform geolocation of the lidar footprint and range determination, followed by determination of instrument calibration constants to produce profiles of attenuated backscatter coefficients. The outputs of the Level 1 algorithms are attenuated backscatter coefficient profiles for the 532 nm and 1064 nm intensity and for the 532 nm perpendicular (cross-polarized) return, along with information on the uncertainties in these products. These data are used by the Level 2 algorithms to produce science data products. In addition, calibration files are generated that track the calibration constants that are determined and applied to the data during Level 1 processing.

The calibration of the 532 nm parallel channel is determined in the usual way by using returns from a high-altitude aerosol free region to compute a backscatter coefficient that is normalized to a molecular backscatter coefficient calculated from a model atmosphere. The 532 nm perpendicular channel is calibrated relative to the 532 nm parallel channel by inserting a pseudo-depolarizer into the 532 nm beam path inside the receiver. The 1064 nm calibration constant is obtained relative to the 532 nm calibration constant using the assumption that the cirrus backscatter is invariant at the two wavelengths. A more detailed description of the Level 1 calibration algorithms can be found in CALIOP Level 1 ATBD (PC-SCI-201).

The Level 2 algorithms are divided into three modules which have the general functions of detecting layers, classifying these layers by type, and performing extinction retrievals. These three modules are the Selective Iterated BoundarY Locator (SIBYL), the Scene Classification Algorithm (SCA), and the Hybrid Extinction Retrieval Algorithms (HERA), respectively. While the layer detection algorithms bear similarities to the LITE feature finder, the addition of a scene classification algorithm to CALIPSO data processing is a major advancement over LITE. SIBYL is adapted to the detection of weak features that lie beneath strong features using a dynamic thresholding scheme [*Vaughan et al.*, 2004]. It estimates layer optical depths, which are then used to correct the profile data for the signal attenuation of overlying features. The primary retrieval of layer optical properties is performed by HERA, however. A detailed description of the feature finder algorithms can be found in the Feature Detection and Layer Properties ATBD (PC-SCI-202 Part 2).

The fundamental algorithms in the CALIPSO analysis framework can be considered as profile processes. These routines are rooted in traditional lidar data analysis techniques, and take as inputs either a single profile of lidar measurements, or, in the case of the layer classification routines, a collection of integrated quantities derived from some segment of a profile. Similarly, the outputs from these profile processes are either a derived profile of optical parameters (e.g., volume extinction coefficients), the integral of such a profile (e.g., optical depth), or some additional information about the content and/or structure of the input profile (e.g., as provided by base and top altitudes). In every case, the uncertainties associated with the outputs of these profile processes are a strong function of the signal-to-noise ratio (SNR) of the input data. Therefore, perhaps the most critical and innovative steps in the CALIPSO analysis framework occur during the scene processes that run immediately prior to the initiation of any of the individual profile processes. These scene processes are essentially sophisticated, multi-level averaging schemes whose function are to identify and extract high SNR profile data from an extended, contiguous sequence of profile measurements; that is, from a lidar "scene". The averaged profiles thus obtained are then delivered for analysis to the appropriate profile processes. Due to the random noise inherent in the signal, the quality of information contained in a single, full resolution backscatter profile can vary enormously, and depends strongly on the scattering intensity of the features being measured. The backscatter intensities within clouds and aerosol layers can range over several orders of magnitude. The detection of the strongest of these features is straightforward, and can be done reliably on a single shot basis. On the other hand, the detection and analysis of the faintest features often requires considerable horizontal and vertical averaging, both to improve feature detection and to ensure the accurate retrieval of feature optical properties. While averaging will increase retrieval accuracies when applied to a homogeneous region, in a heterogeneous scene it can smear or eliminate important structural variability within features, and can irretrievably intermingle the signals from both aerosols and clouds into a single profile, thus degrading the information content of the measurements. Therefore, in addition to these profile processes, a set of fully automated "scene processes" have been designed to intelligently extract suitably averaged data from contiguous lidar profiles. The sections below describe the scene processes developed for layer detection and the subsequent optical analyses.

The Scene Classification Algorithm first identifies layers as either cloud or aerosol, based primarily on scattering strength and the spectral dependence of the lidar backscattering. The algorithm is based on the use of probability distribution functions (PDFs) of 532-nm attenuated backscatter coefficients, and of the ratio of the 532-nm and 1064-nm attenuated backscatter [*Liu et al.*, 2004]. This latter quantity is referred to as the attenuated color ratio, χ'. If a layer is classified as cloud, the SCA will then determine if it is an ice cloud or water cloud using the layer-average depolarization ratio, along with ancillary information such as layer height and temperature [*Hu et al.*, 2001]. The SCA also uses a combination of observed parameters and *a priori* information to select an appropriate extinction-to-backscatter ratio, or lidar ratio (S_a for aerosol layers, S_c for clouds), and multiple scattering function, $\eta(z)$, required for retrieving extinction and optical depth. The lidar ratios and multiple scattering functions are based on the same underlying aerosol or cloud particle model. A detailed description of the scene classification algorithm can be found in the Scene Classification ATBD (PC-SCI-202 Part 3).

The subsequent tasks of computing final estimates of optical depth, and extracting profiles of particulate backscatter and extinction coefficients are carried out by the HERA module [*Young et*

al., 2004]. HERA is a hybrid collection of procedures that have been combined to form a single, fully automated scene process responsible for retrieving profiles of optical properties from the features identified by SIBYL. The constituent algorithms include a routine that averages varying numbers of profiles on the SIBYL spatial grid to produce a single attenuated backscatter profile that is subsequently used by the layer classification algorithms and the extinction retrieval algorithms. Whereas SIBYL makes an initial estimate of the transmittance loss at 532-nm through a feature for the purpose of correcting the underlying signals for this attenuation, HERA calculates and corrects for attenuation within all features in order to produce profiles of extinction and backscatter at both 532 nm and 1064 nm. HERA corrects for attenuation effects beneath all features, including those where SIBYL is unable to make an accurate assessment of the feature transmittance (e.g. where the SNR is too low). A detailed description of the HERA algorithms can be found in the Extinction Retrieval and Particle Properties ATBD (PC-SCI-202 Part 4).

6. CALIOP Calibration Processing

The Level 1 calibration algorithms are designed to accomplish two major goals: (1) the determination of calibration constants for the three lidar channels, and (2) the application of those calibration constants to produce profiles of attenuated backscatter coefficients to be used in the Level 2 processing. An overview of the Level 1 calibration processing architecture is shown in Figure 6.1 and described below.

Determination of the calibration constants is a three-step process applied to the geolocated profiles:

(a) The calibration constant is first determined for the 532-nm parallel channel. This is done by comparing the measured 532-nm parallel channel signal from the 30-34 km region to an estimate of the parallel backscatter coefficient computed from a modeled atmospheric density profile. The 30-34 km altitude is chosen because there is little aerosol at that height and the backscatter is primarily molecular. The estimated backscatter is calculated from the molecular number density and the backscatter cross section of dry air.

(b) The calibration of the 532-nm parallel channel is then transferred to the perpendicular channel. There is not enough signal to calibrate the perpendicular channel by comparing the signal to the expected backscatter coefficient in the mid-stratosphere, as is done for the parallel channel, due to the fact that molecular depolarization is less than 1%. Instead, the relative calibration of the perpendicular channel with respect to the parallel channel is determined using data collected during the Polarization Gain Ratio (PGR) operation. During this operation, a pseudo depolarizer is inserted into the optical path of the 532-nm channel upstream of the polarizing beam splitter. The pseudo depolarizer insures that equal optical signal levels are directed to the parallel and perpendicular detectors, enabling a calculation of the relative gains between those two channels.

(c) Calibration of the 532nm parallel and perpendicular channels is then transferred to the 1064-nm channel. As with the 532-nm perpendicular channel, the signal from the 1064-nm channel in the mid-stratosphere is too low to provide a reliable calibration measurement. Transfer of calibration from the 532-nm channels to the 1064-nm channels is accomplished using the backscatter from cirrus clouds. Because cirrus cloud particles are large with respect to the laser wavelengths, the ratio of the 532-nm and 1064-nm cirrus extinction

coefficients is known to be approximately 1.0 and the ratio of the 532-nm and 1064-nm cirrus backscatter coefficients is essentially constant throughout a layer. The 1064-nm calibration constant is thus determined by comparing the 1064-nm backscatter signal with the calibrated 532-nm cirrus backscatter measurements.

These three steps are described in detail in the Calibration and Level 1 Data Products ATBD (PC-SCI-201).

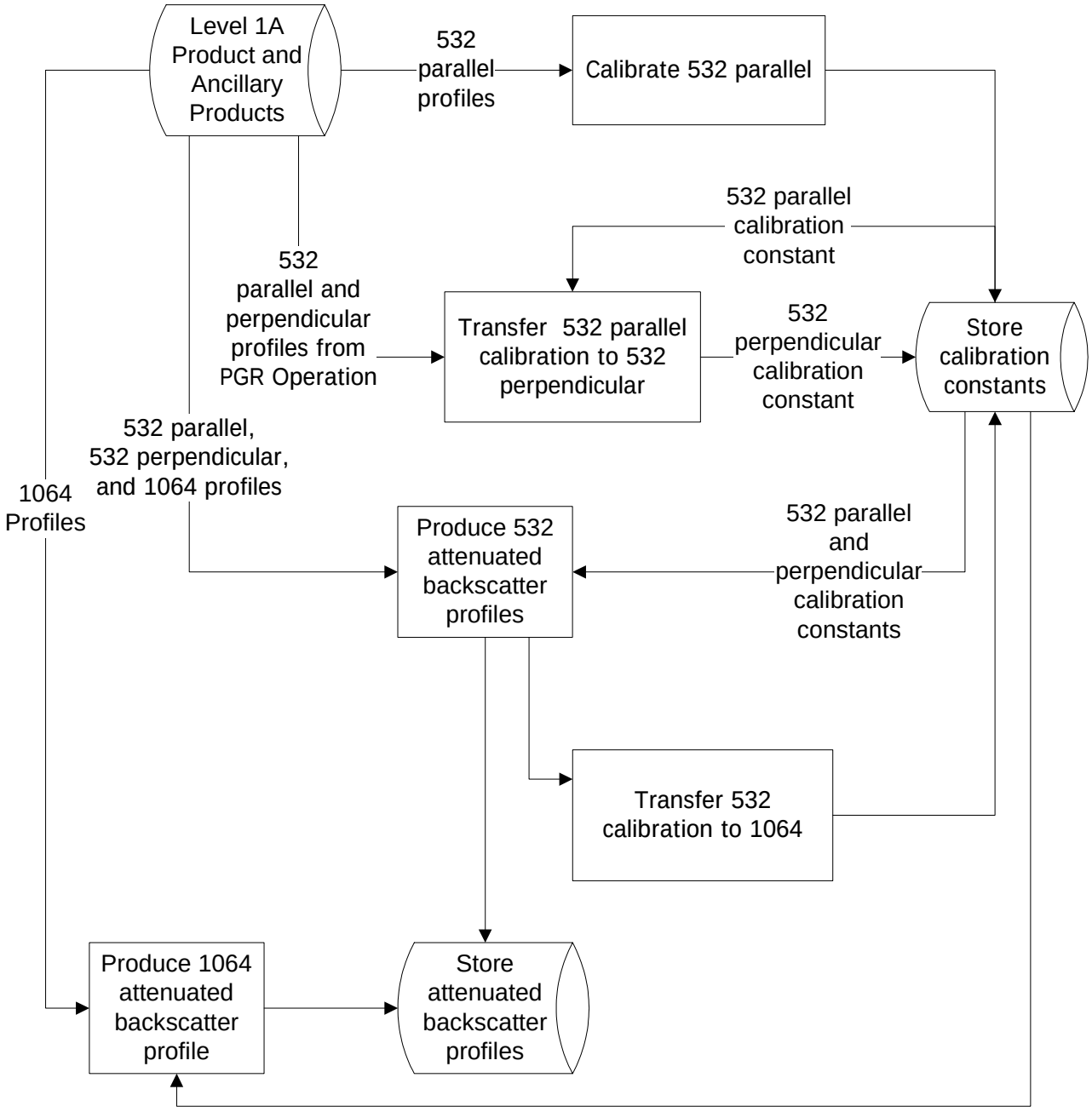

Figure 6.1. Block diagram representing the basic flow of the Level 1B processes

6.1. General Form of the Lidar Equation

Prior to Level 1 calibration processing, the lidar signal has been corrected for offset voltages, background signals, and instrument artifacts. The resulting signal to be calibrated can be written as

$$P(r) = \frac{1}{r^2} E_0 \, \xi \, \beta(r) \, T^2(r) \ , \tag{6.1}$$

where

$$T^2(r) = \exp\left[-2 \int_0^r \sigma(r') \, dr' \right], \tag{6.2}$$

and

r	=	range from the satellite to the sampled volume,
$P(r)$	=	measured signal after background subtraction and artifact removal,
E_0	=	average laser energy for the single-shot or composite profile,
ξ	=	lidar system parameter,
$\beta(r)$	=	volume backscatter coefficient at range r,
$T(r)$	=	one-way transmittance (i.e., signal attenuation) from the lidar to the scattering volume at range r, and
$\sigma(r)$	=	volume extinction coefficient at range r.

In analyzing the data, we work either with profiles composed of returns from a single laser shot or returns composed from the average of several laser shots. The parameters in the lidar equation may change from profile to profile, and we indicate this explicitly with a profile index, k, as follows

$$P(r,k) = \frac{1}{r^2} E_0(k) \, \xi(k) \, \beta(r,k) \, T^2(r,k) \ . \tag{6.3}$$

The signal is written in terms of the range from the satellite, r; however, this notation can lead to confusion. The atmospheric parameters, β and σ, are more appropriately considered functions of altitude, z, above mean sea level. The one-way transmittance is a function of optical path length through the attenuating atmospheric volume above the scattering volume and hence it can be considered as a function of either altitude or range. The distinction is insignificant if the lidar is pointed directly at nadir. For significant deviations from nadir pointing, the equation is recast in more explicit terms as

$$P(z,k,\theta) = \left(\frac{\cos(\theta)}{z_{sat}(k) - z} \right)^2 E_0(k) \ \xi(k) \ \beta(z,k) \exp\left[-2 \int_0^r \sigma\left(z(r',k), k \right) dr' \right], \tag{6.4}$$

where

$$z(r,k) = z_{sat}(k) - r \cos\left(\theta(k)\right), \tag{6.5}$$

and

$\theta(k)$	=	average off-nadir angle for the k^{th} laser shot or composite profile; and

$z_{sat}(k)$ = average altitude of the satellite for the k^{th} laser shot or composite profile.

The nominal off-nadir angle for the CALIPSO mission is 0.3˚, and for this small value the correction for the cosine of the angle is insignificant. However, if the system is pointed significantly off-nadir, the cosine angle correction can be important.

6.2. Lidar System Parameter and Calibration Factor

The lidar system parameter is the product of a number of instrument parameters that govern the sensitivity and efficiency of the lidar. Factors making up the lidar system parameter include the receiver area, the receiver optical efficiency, the detector sensitivity, the electronic gain in the detection electronics, and the geometric overlap between the laser footprint and the receiver field of view (boresight overlap). Many of these factors can vary over time. Some of this temporal variability is in response to commanded and autonomous instrument operations while the remainder is due to non-ideal instrument effects. Examples of commanded changes include changes in amplifier gain and offset. The amplifier gain and offset are changed twice per orbit to accommodate changing lighting conditions as the spacecraft crosses the terminator. Examples of non-ideal instrument effects include changes in detector sensitivity and boresight drift. The detector sensitivity is expected to change gradually over the course of the mission due to degradation of the detectors. The boresight overlap may change slowly due to subtle thermal/mechanical effects. Amplifier gains have been well characterized prior to launch and changes in the gain are accounted for in post processing. Other components of the lidar system parameter must be measured during the on-orbit calibration process.

In processing the data, we separate the lidar system parameter into two factors that are accounted for separately:

$$\xi(k) = G_A(k)\ C(k), \tag{6.6}$$

where

$G_A(k)$ = amplifier gain in effect for profile k, and

$C(k)$ = lidar calibration factor.

The amplifiers are commanded to one of a discrete set of values, which are determined prior to launch, hence the amplifier gain is known and is downlinked with the data.

6.3. Level 1 Profile Product Description

The profile products produced in Level 1 processing are range-scaled, energy normalized, gain-normalized and calibrated versions of the signal, P. The Level 1 profile product can be written as

$$\beta'(z,k) = \frac{r^2\ P(r,z)}{E(k)\ G_A(k)\ C(k)} = \beta(z,k)\ T^2(z,\theta,k) \tag{6.7}$$

To make the equations less cumbersome, we simplify the notation as follows

$$\beta'(z) = \beta(z)\ T^2(z) \tag{6.8}$$

while maintaining an understanding of the implicit dependencies on profile index and off-nadir angle.

The Level 1 data product contains profile products for the three lidar channels. The attenuated backscatter coefficients for the 532-nm parallel, 532-nm perpendicular, and 1064-nm channels are defined, respectively, as follows.

$$\beta'_{532,\parallel}(z) = \beta_{532,\parallel}(z)\, T_{532}{}^{2}(z) \tag{6.9}$$

$$\beta'_{532,\perp}(z) = \beta_{532,\perp}(z)\, T_{532}{}^{2}(z) \tag{6.10}$$

$$\beta'_{1064}(z) = \beta_{1064}(z)\, T_{1064}{}^{2}(z) \tag{6.11}$$

The Level 1 data product reports profiles of the 532-nm total attenuated backscatter coefficients (i.e., $\beta'_{532,total}(z) = \beta'_{532,\parallel}(z) + \beta'_{532,\perp}(z)$), the 532-nm perpendicular attenuated backscatter coefficients (i.e., as given by equation (6.10)), and the 1064-nm total attenuated backscatter coefficients (i.e., as given by equation (6.11)).

7. CALIOP Level 2 Data Analysis

In this section we present a brief summary of the design of the lidar Level 2 algorithms. The primary data parameters produced by the lidar Level 2 subsystem are:

- layer heights and descriptive properties (e.g., integrated attenuated backscatter, layer integrated depolarization ratio, etc.);
- layer identification and typing (i.e., cloud vs. aerosol, ice cloud vs. water cloud, etc.); and
- profiles of cloud and aerosol backscatter and extinction coefficients.

The input data required by the CALIOP Level 2 subsystem are:

- calibrated profiles of attenuated backscatter at 1064 nm (obtained from the Level 1 subsystem);
- calibrated profiles of 532-nm parallel-polarized attenuated backscatter (obtained from the Level 1 subsystem);
- calibrated profiles of 532-nm perpendicular-polarized attenuated backscatter (obtained from the Level 1 subsystem); and
- ancillary geophysical and meteorological data such as surface elevation and profiles of temperature and pressure (obtained from the ancillary data server).

Before the retrieval of extinction coefficients can be performed, clouds must be located and discriminated from aerosol, and water clouds must be discriminated from ice clouds. In the Level 2 algorithms, the Selective Iterated BoundarY Locator (SIBYL) detects layers, the Scene Classification Algorithm (SCA) classifies these layers, and the Hybrid Extinction Retrieval Algorithms (HERA) perform extinction retrievals. Although the location of cloud and aerosol layers and the determination of cloud ice/water phase are necessary precursors to extinction retrieval, these data products are of interest in their own right.

The high level flow of the Level 2 algorithms and the data products they produce is outlined in Figure 7.1. The output from the CALIOP Level 2 processing system falls into several major types of products. Final products are reported at uniform spatial resolutions, which are derived via averaging and/or interpolation from the varying resolutions used in generating the intermediate products. These are the Level 2 products intended for use by the science community. The three CALIOP Level 2 modules are discussed in detail in the following three sections

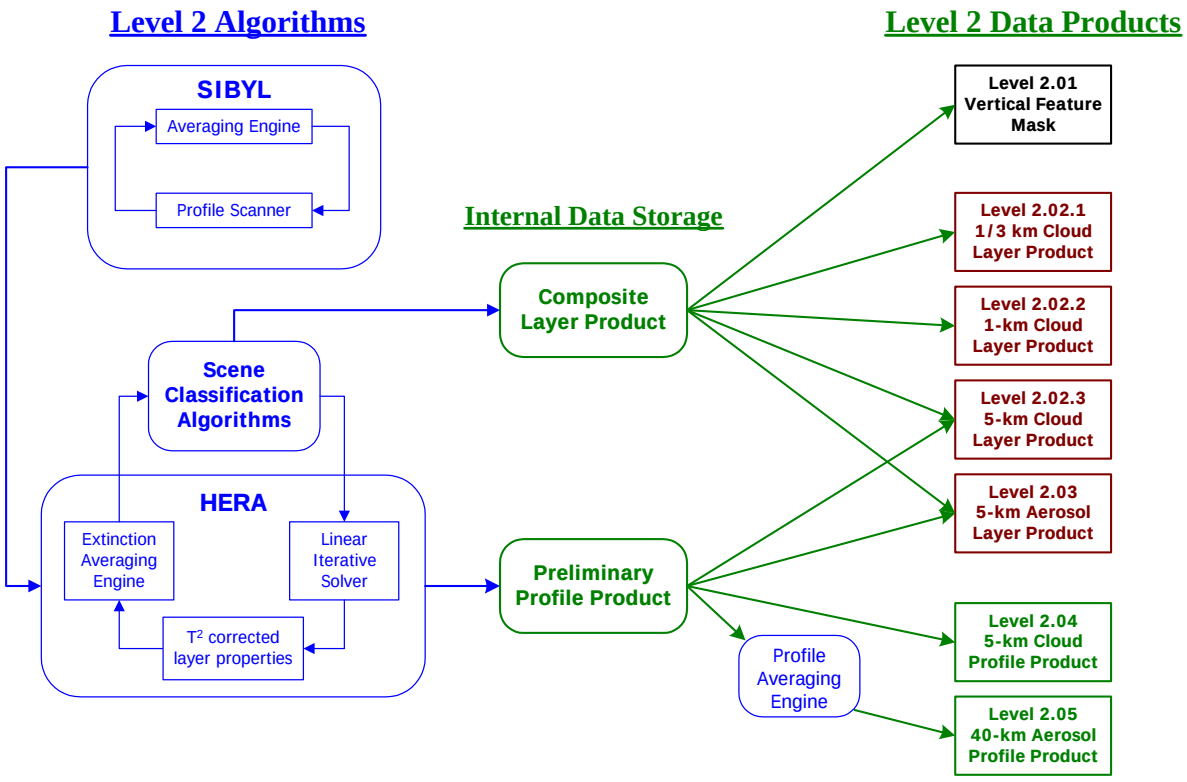

Figure 7.1 Level 2 Algorithms and Data Products

.

7.1. Selective Iterated Boundary Locator (SIBYL)

The first processing step is to locate identifiable layers, whether they are cloud or aerosol. Because the natural variation of backscattering coefficients is very large, a "profile scanner" is used to find layers repeatedly on several passes through the data. This algorithm is based on one developed for detecting cloud and aerosol layers in LITE data [*Platt et al.*, 1999]. The algorithm has been tested using LITE data converted to simulated CALIPSO data [*Vaughan et al.*, 2002].

Dense clouds can be detected using single-shot data, but tenuous clouds and most aerosols require the lidar profiles to be averaged to increase SNR and allow weaker layers to be detected. For example consider the scenario in Figure 7.2, a color-modulated plot of the 532-nm backscatter signal of LITE data and single shot profile plots of three selected regions. The plot on the left is a single shot profile of faint cirrus overlying a PBL aerosol layer. The middle plot

shows thin cirrus and aerosol layers, and the plot on the right shows strong cirrus overlying stratus clouds. The single shot profiles show the degree to which strong and weak features are intermingled. The spatial resolution of the features found by SIBYL will therefore depend on the intensity of the feature; i.e., strong features are be reported at a higher resolution than weak features.

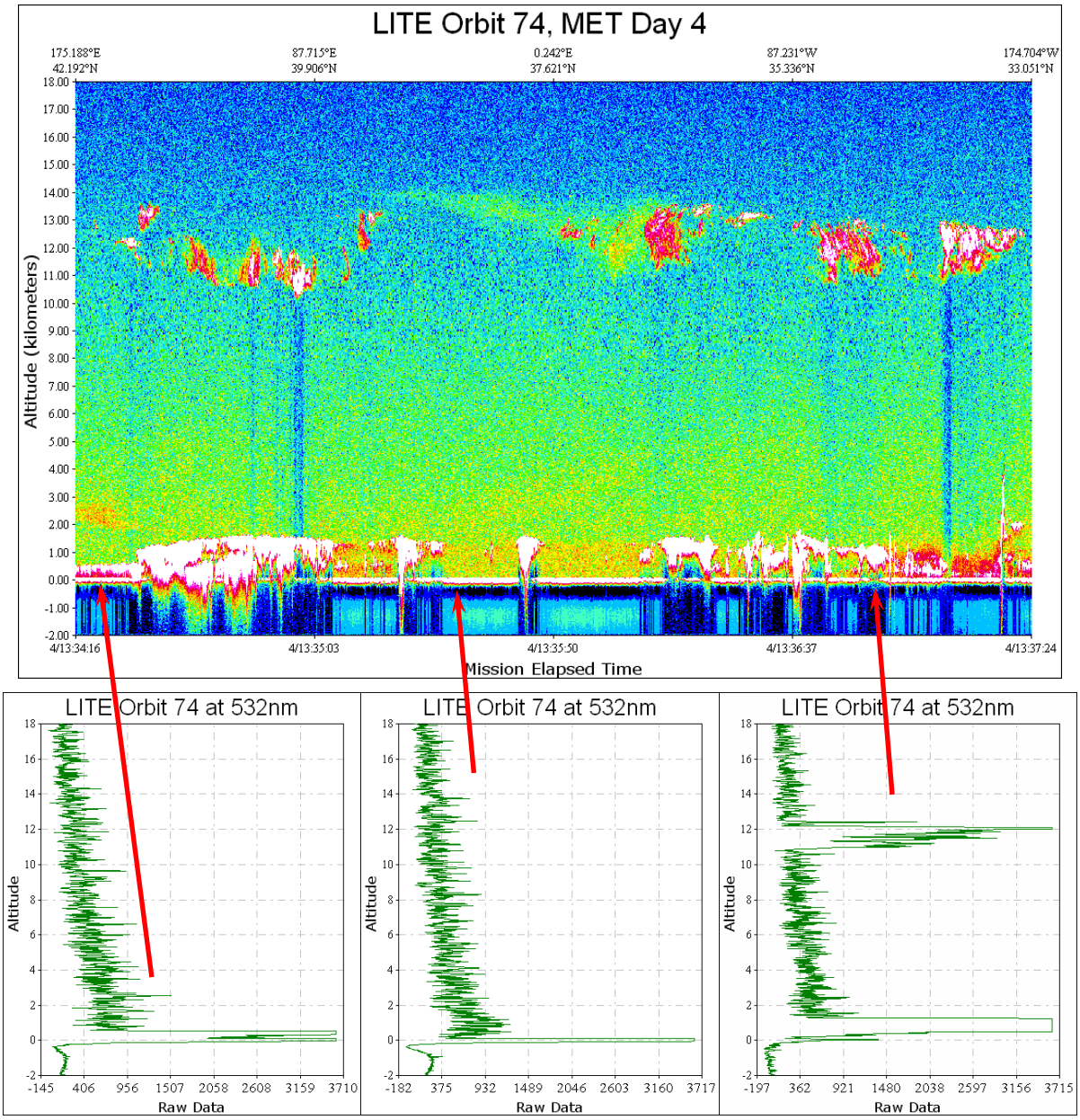

Figure 7.2 Color-modulated plot of the backscattering signal from 532-nm channel of the LITE data and singleshot profile plots of the regions indicated by arrows.

The strongest features can be identified in single-shot profiles and removed. Cloud clearing prior to averaging, as shown in Figure 7.3, produces averaged aerosol profiles which are not contaminated by cloud. After strong features are found at the highest spatial resolution, the remaining profile data are averaged to allow weaker features to be found. Making several passes through the data with successively greater averaging allows strong features to be found at high spatial resolution and locates weaker layers at the best possible spatial resolution. The spatial averaging intervals used by SIBYL are driven in part by the requirements of the extinction retrieval algorithm, which requires a certain level of averaging (i.e., a minimum SNR) to avoid retrieval biases. A detailed, illustrated description of SIBYL's nested, multi-grid averaging scheme is given in the feature finder ATBD (PC-SCI-202, Part 2).

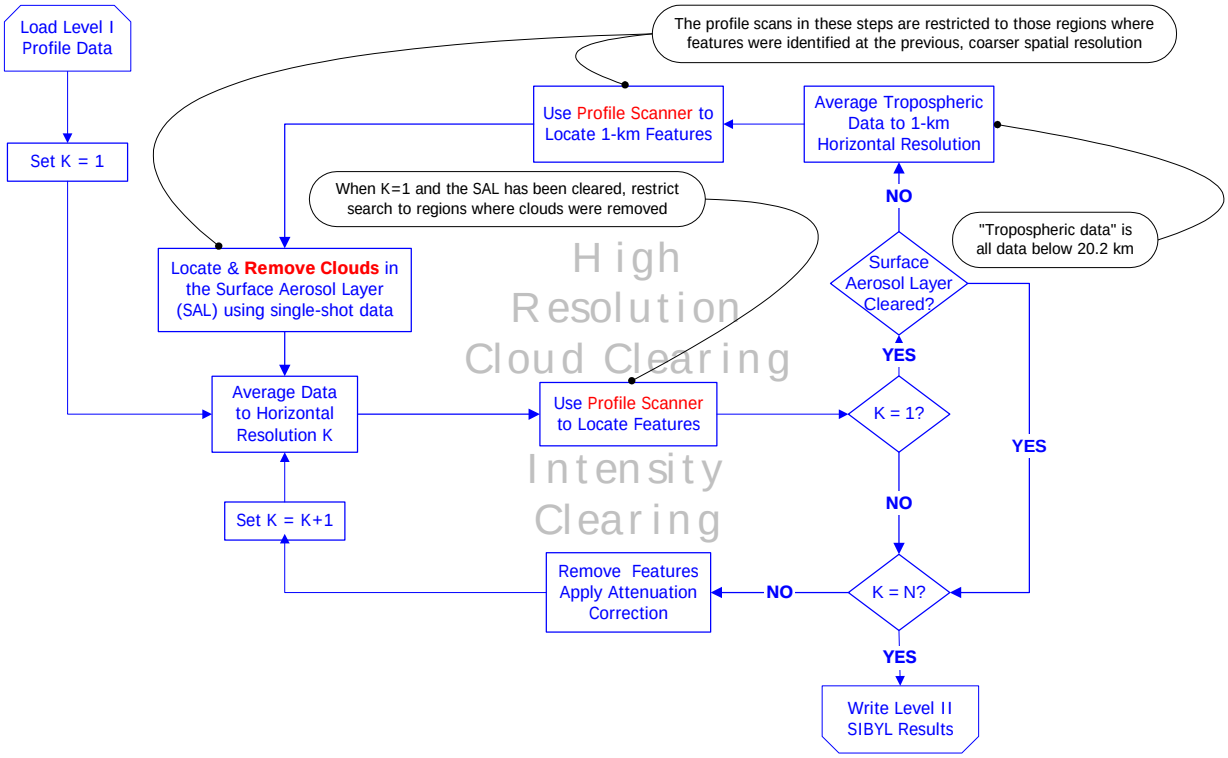

Figure 7.3 High level schematic of the Selective Iterated BoundarY Locator (SIBYL) module.

In the process of finding layers, a number of other quantities are computed such as transmittance of non-opaque layers embedded in clear air, and layer-integrated signal backscatter. Some of these quantities are used later by the classification and extinction retrieval algorithms.

7.2. Scene Classification Algorithms (SCA)

The Scene Classification Algorithms (SCA) consist of a family of algorithms which perform several functions to identify the features found by SIBYL. The individual algorithms conduct tests based on a set of "layer descriptors", which provide fundamental spatial, temporal, and optical characteristics of the feature. These layer descriptors are computed either by SIBYL or within the SCA. Once the results of these tests have been computed, the SCA evaluates them

and makes classification decisions accordingly. Along with each classification, the SCA also computes a confidence flag, which indicates the level of confidence of the classification.

A schematic of the scene classification tasks is shown in Figure 7.4. The SCA first identifies layers as either cloud or aerosol, based primarily on scattering strength and the spectral dependence of backscattering. The SCA computes the depolarization profile within layers using the Level 1 532 nm parallel and perpendicular profiles. Cloud layers are then classified as ice or water, primarily using the depolarization signal and the temperature profile supplied as part of the ancillary data. Aerosol layers are similarly distinguished according to type using indicators such as depolarization, geophysical location, and backscatter intensity. Based on this classification according to type, the SCA then estimates values of the lidar ratio, S, for clouds and aerosols, and selects the appropriate range-dependent multiple scattering correction function, $\eta(z)$, for the layer. The cloud/aerosol and cloud ice/water phase determinations are required output data products. The values determined for lidar ratio and the associated $\eta(z)$ are then passed on to HERA.

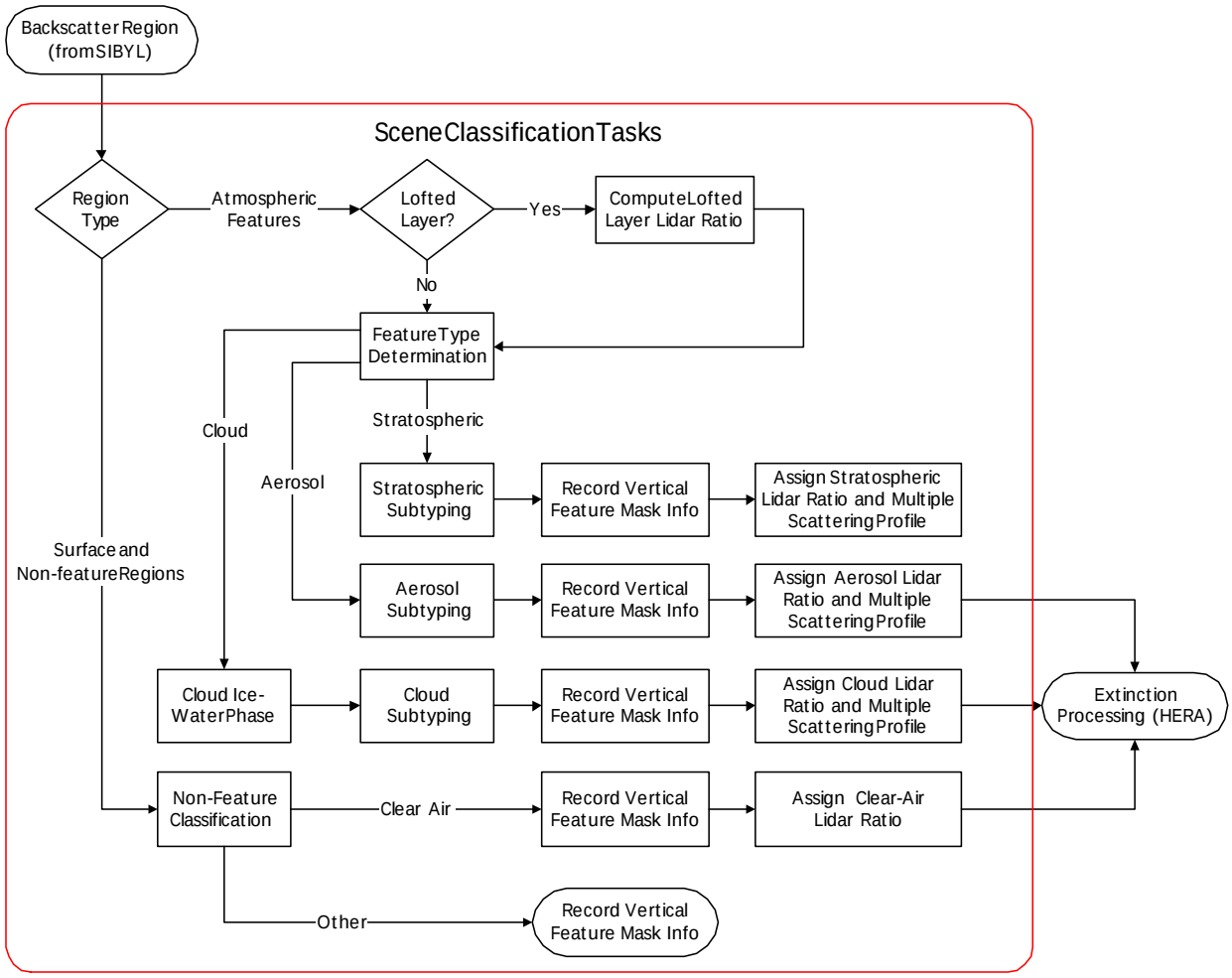

Figure 7.4 Schematic of the Scene Classification Algorithm (SCA).

CALIOP has the sensitivity to observe polar stratospheric clouds and volcanic plumes which reach the stratosphere. Currently, features found in the stratosphere are labeled as stratospheric

features and are not classified further. Presently, aerosol loading in the stratosphere is very low and the background stratospheric aerosol is expected to be undetectable by CALIPSO.

7.3. Hybrid Extinction Retrieval Algorithms (HERA)

The Hybrid Extinction Retrieval Algorithm (HERA) performs extinction retrievals on regions of profile data identified by SIBYL, using lidar ratios and multiple scattering factors supplied by the SCA. Figure 7.5 shows a schematic of the algorithm. HERA incorporates a sophisticated retrieval engine which extracts profiles of particulate backscatter and extinction coefficients from the profiles of attenuated backscatter coefficients identified as layers by SIBYL. During the solution process, HERA explicitly includes multiple scattering effects. These retrievals produce profiles of particulate backscatter and extinction at both 532 nm and 1064 nm. HERA autonomously decides among a number of options how to best perform the retrieval of each feature identified by SIBYL, depending on the turbidity of the layer and whether or not the layer is bounded above and below by regions of clear air. To provide a complete profile of aerosol backscatter, HERA also performs retrievals in the regions of the atmosphere where no features have been found (i.e., in clear air). Because SIBYL detects layers on several passes through the data with increasingly greater averaging, the profile data ingested into HERA does not have a uniform spatial resolution. HERA performs retrievals on each profile segment using the same averaging intervals required for detection by the SIBYL module, and thus the profiles of extinction and backscatter initially produced by HERA may also have varying spatial resolution. While HERA's native output is spatially inhomogeneous, the data products distributed to the users are partitioned into separate cloud and aerosol products, each of which is mapped onto a uniform spatial grid.

The ultimate goal is to retrieve extinction and backscatter profiles of all cloud layers at the highest possible spatial resolution, and comprehensive profiles of aerosol extinction and backscatter. Following the retrieval of extinction profiles, a number of other parameters are computed by HERA using the profiles of extinction and attenuation-corrected backscatter. These parameters include: optical depth, particle (cloud or aerosol) color ratio, and particle depolarization ratio.

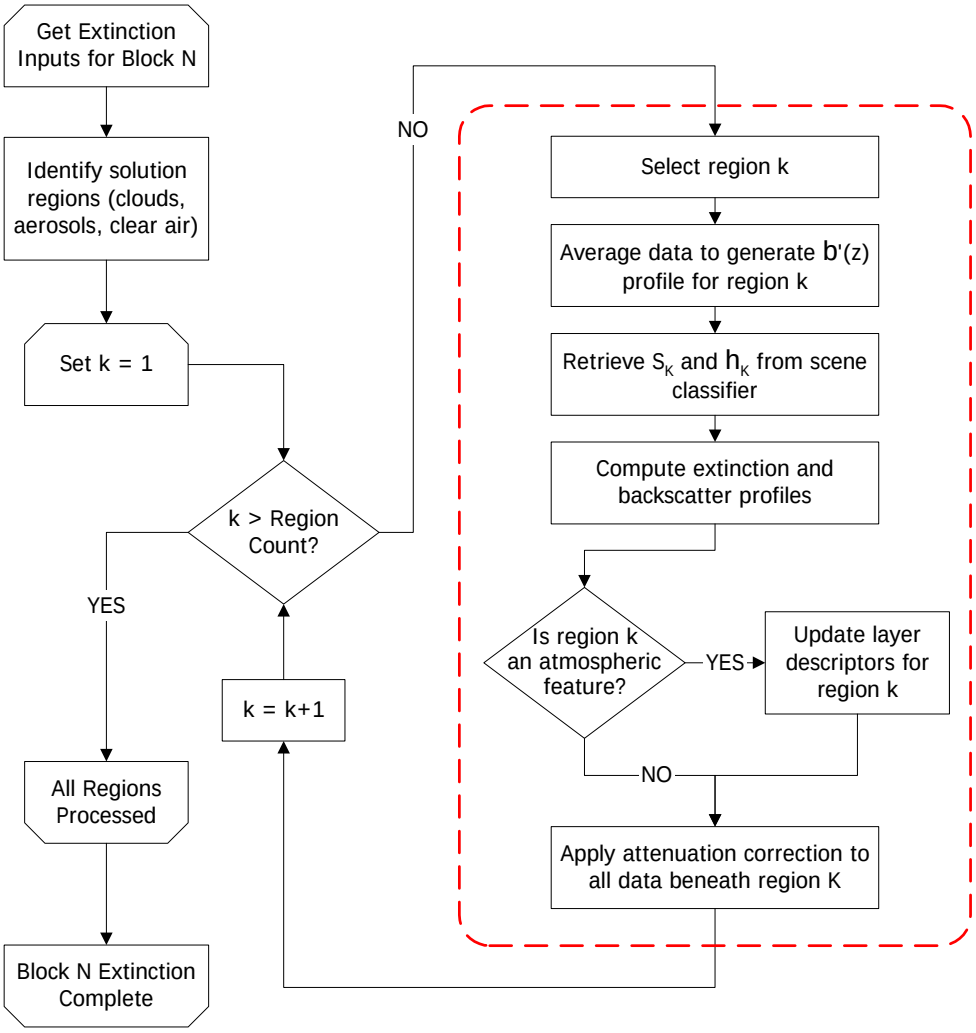

Figure 7.5 A schematic of the HERA module

7.4. Supporting Topics

The CALIOP Level 2 ATBD is divided into several parts covering particular aspects of the algorithms which deserve an extended discussion. Part II of the ATBD gives a detailed description of the feature detection and layer properties algorithms, while Parts III and IV cover in detail the SCA and HERA modules, respectively. Part V describes the data formats of the vertical feature mask, and the cloud and aerosol layer and profile products.

Additional information, e.g., the rationale for selection of the lidar ratio for clouds and aerosols, and the treatment of multiple scattering, can be found in various publications listed on the CALIPSO publications site at http://www-calipso.larc.nasa.gov/resources/publications.php. A full listing of the parameters produced by the CALIOP Level 2 subsystem and their organization into data products is provided in the Data Products Catalog (doc. no. PCI-SCI-503). Data parameters are be described in Data Product User Guides.

8. References

Cess, R.D., M.H. Zhang, P. Minnis, L. Corsetti, E.G. Dutton, B.W. Forgan, D.P. Garber, W.L. Gates, J.J. Hack, E.F. Harrison, X. Jing, J.T. Kiehl, C.N. Long, J.-J. Morcrette, G.L. Potter, V. Ramanathan, B. Subasilar, C.H. Whitlock, D.F. Young, and Y. Zhou, Absorption of solar radiation by clouds: Observation versus models, *Science*, *267* (Jan 95), 496-499, 1995

Elterman, L., Aerosol measurements in the troposphere and stratosphere, *Applied Optics*, *5*, 1769-1776, 1966

Fernald, F.G., Analysis of atmospheric lidar observations: some comments, *Applied Optics*, *23*, 652-653, 1984

Fouquart, Y., J.C. Buriez, M. Herman, and R.S. Kandel, The influence of clouds on radiation: A climate-modeling perspective, *Rev. Geophys.*, *28*, 145-166, 1990

Hu, Y.-X., D. Winker, P. Yang, B. Baum, L. Poole, and L. Vann, Identification of cloud phase from PICASSO-CENA lidar depolarization: A multiple scattering sensitivity study, *J. Quant. Spectros. Radiat. Trans.*, *70*, 569-579, 2001

IPCC, *Climate Change 2001: The Scientific Basis: Contribution of Working Group I to the Third Assessment Report of the Intergovernmental Panel on Climate Change (IPCC)*, 944 pp., Cambridge University Press, Cambridge, UK, 2001.

Klett, J.D., Lidar inversion with variable backscatter/extinction ratios",, *Applied Optics,*, *24*, 1638-1643,, 1985

Liu, Z., M.A. Vaughan, D.M. Winker, C.A. Hostetler, L.R. Poole, D.L. Hlavka, W.D. Hart, and M. J. McGill, Use of Probability Distribution Functions for Discriminating Between Cloud and Aerosol in Lidar Backscatter Data, *Journal of Geophysical Research.*, *109*, 2004,doi:10.1029/2004JD004732, 2004.

McGuire, J.P., and R.A. Chapman, Analysis of spatial pseudo depolarizers in imaging systems, *Opt. Eng.*, *29*, 1478-1484, 1990

Omar, A.H., D.M. Winker, and J.-G. Won, Aerosol Models for the CALIPSO Lidar Inversion Algorithms, in *SPIE*, edited by C. Werner, pp. 104-115, Deutsches Zentrum fuer Luft- und Raumfahrt e.V. (Germany), Barcelona, Spain, 2004.

Omar, A.H., J.-G. Won, D.M. Winker, S.-C. Yoon, O. Dubovik, and M.P. McCormick, Development of global aerosol models using cluster analysis of Aerosol Robotic Network (AERONET) measurements, *J. Geophys. Res.*, *110* (D10S14), 2005,doi:10.1029/2004JD004874.

Platt, C.M.R., Lidar and Radiometric Observations of Cirrus Clouds, *J. Atmos. Sci.,, 30*, 1191-1204, 1973

Platt, C.M.R., D.M. Winker, M.A. Vaughan, and S.D. Miller, Backscatter-to-extinction ratios in the top layer of tropical mesoscale convective systems and in isolated cirrus from LITE observations, *Journal of Applied Meteorology, 38*, 1330-1345, 1999

Platt, C.M.R., S.A. Young, P.J. Manson, G.R. Patterson, S.C. Marsden, R.T. Austin, and J.H. Churnside, The Optical Properties of Equatorial Cirrus from Observations in the ARM Pilot Radiation Observation Experiment, *J. Atmos. Sci.,*, 1977-1996, 1998

Slingo, A., Sensitivity of the Earth's radiation budget to changes in low clouds, *Letts. Nature, 343* (6253), 49-51, 1990,10.1038/343049a0.

Twomey, S., *Anthropogenic Aerosols*, Elsivier, New York, 1977.

Vaughan, M., S. Young, D. Winker, K. Powell, A. Omar, Z. Liu, Y. Hu, and C. Hostetler, Fully automated analysis of space-based lidar data: an overview of the CALIPSO retrieval algorithms and data products, in *SPIE Int. Soc. Opt. Eng.*, edited by U. Singh, pp. 16-30, Maspalamos, Gran Canaria, Spain, 2004.

Vaughan, M.A., D.M. Winker, and C.A. Hostetler, SIBYL: A selective iterated boundary location algorithm for finding cloud and aerosol layers in CALIPSO lidar data, in *21st International Laser Radar Conference*, edited by L. Bissonette, G. Roy, and G. Vallee, pp. 791-794, Defence R&D, Quebec, Canada, 2002.

Wielicki, B.A., E.F. Harrison, R.D. Cess, M.D. King, and D.A. Randall, Mission to Planet Earth: Role of Clouds and Radiation in Climate, *Bulletin of the American Meteorological Society, 76* (11), 2125-2153, 1995

Winker, D.M., R.H. Couch, and M.P. McCormick, An Overview of LITE: NASA's Lidar In-Space Technology Experiment, *Proceedings of the IEEE, 84* (2), 164-180, 1996

Winker, D.M., W.H. Hunt, and C.A. Hostetler, Status and Performance of the CALIOP Lidar, in *SPIE Int. Soc. Opt. Eng.*, edited by U.N. Singh, pp. 8-15, SPIE, Maspalomas, Gran Canaria, Spain, 2004.

Winker, D.M., and M.V. Vaughan, Vertical distribution of clouds over Hampton, Virginia observed by lidar under the ECLIPS and FIRE ETO programs, *Atmospheric Research, 34*, 117-133, 1994

Young, S.A., Analysis of lidar backscatter profiles in optically thin clouds, *Applied Optics, 34* (30), 7019-7031, 1995

Young, S.A., D.M. Winker, M.A. Vaughan, and K.A. Powell, The retrieval of extinction profiles in optically-inhomogeneous cloud and aerosol layers detected by the CALIPSO lidar, in *22nd International Laser Radar Conference(ILRC 2004)*, edited by G. Pappalardo, and A. Amodeo, pp. 999-1002, ESA, Matera, Italy, 2004.

Zwally, H.J., B. Schutz, W. Abdalati, J. Abshire, C. Bentley, A. Brenner, J. Bufton, J. Dezio, D. Hancock, D. Harding, T. Herring, B. Minster, K. Quinn, S. Palm, J. Spinhirne, and R. Thomas, ICESat's laser measurements of polar ice, atmosphere, ocean, and land, *J. Geodynamics*, *34*, 405-445, 2002